SCIENCE CHINA
Earth Sciences

• RESEARCH PAPER •

February 2010 Vol.53 No.2: 189–202
doi: 10.1007/s11430-010-0001-7

Conductivity structure and rheological property of lithosphere in Southern Tibet inferred from super-broadband magnetotelluric sounding

WEI WenBo[1,2,3*], JIN Sheng[1,3], YE GaoFeng[1,3], DENG Ming[1,3], JING JianEn[1,3], Martyn UNSWORTH[4] & Alan G. JONES[5]

[1] *Key Laboratory of Geo-detection of Ministry of Education, Beijing 100083, China;*
[2] *State Key Laboratory of Geological Processes and Mineral Resources, Beijing 100083, China;*
[3] *School of Geophysics and Information Technology, China University of Geosciences, Beijing 100083, China;*
[4] *Department of Physics, University of Alberta, Edmonton, Alberta T6G, 2J1, Canada;*
[5] *School of Cosmic Physics, Dublin Institute of Advanced Studies, 5 Merrion Square, Dublin 2, Ireland*

Received December 15, 2008; accepted May 27, 2009; published online January 2, 2010

To understand deep lithosphere structure beneath the Qinghai-Tibet Plateau more comprehensively and objectively and to explore important scientific issues, such as characteristics of plateau lithospheric deformation, state of strain, thermal structure, plate (or terrane) movement, and crust-mantle rheology, it is necessary to research the variation of crust-mantle electrical structure in the east-west direction in every geological unit. For this purpose, six super-broadband magnetotelluric (MT) sounding profiles have been completed by INDEPTH-MT Project in the Himalayas-Southern Tibet. Based on the imaging results from the six profiles, three-dimensional electrical conductivity structure of the crust and upper mantle has been analyzed for the research area. The result shows that the high-conductivity layers in the middle and lower crust exist widely in Southern Tibet, which extend discontinuously for more than 1000 km in the east-west direction and become thinner, shallower and more resistive toward the big turning of the Yarlung Zangbo River. The discussion on the rheology of lithosphere in Southern Tibet suggests that the mid-lower crust there is of high electrical conductivity, implying the existence of "partial-melt" and "hot fluid" in the thick crust of Tibet, which make the medium hot, soft, and plastic, or even able to flow. Combining the experimental result of petrophysics and the MT data, we estimate the melting percentage of the crustal material to be up to 5%–14%, which would reduce the viscosity of aplite in the crust to meet the flow condition; but for granite, it is likely not enough to cause such a change in rheology.

Southern Tibet, super-broadband magnetotelluric sounding, crust, electrical conductivity, rheological property

Citation: Wei W B, Jin S, Ye G F, et al. Conductivity structure and rheological property of lithosphere in Southern Tibet Inferred from super-broadband magnetotelluric sounding. Sci China Earth Sci, 2010, 53: 189−202, doi: 10.1007/s11430-010-0001-7

Since 1992, a co-operative project among geologists and geophysicists of People's Republic of China and the United States of America was initiated in Tibet. It focused on imaging the fine structure of the crust by the use of near-vertical seismic deep reflection method. This effort is called International Deep Profiling of Tibet and the Himalaya (INDEPTH).

The result of INDEPTH (I) has revealed a clear detachment surface, on which the India Plate underthrusts beneath the Eurasia Plate, as well as the Moho interface [1]. It proves that the new generation of geophysical methods can make significant contributions to the probing of deep struc-

*Corresponding author (email: wwb5130@cugb.edu.cn)

ture of the Tibetan Plateau. In 1995, INDEPTH (II) was expanded to include magnetotelluric sounding (INDEPTH-MT), which was a joint effort among the scientists of China University of Geosciences (Beijing), Washington University of US (Seattle), and Geological Survey of Canada. Its objective is to explore conductivity of the crust of Tibet, which is associated with thermal structure and rheology of the lithosphere there. By 1997, three super-broadband (320–0.00005 Hz) MT profiles were completed, which are Yatung-Xoggola (line 100), Taktse-Bamucuo (line 200), and Xoggola-Damshung (line 300) [2–4]. The subsequent INDETH (III)-MT in 1998 and 1999 completed another two profiles, i.e., Dechen-Longweico (line 500) and Nakchu-Golmud (line 600) [5–7].

The interpretation of these new data suggests that partially molten layers probably exist in the crust of Southern Tibet as indicated by anomalies of high conductivity there. Further analysis shows that the mid-lower crust at the depth of tens of kilometers between Khangmar and the Kunlun Mountains is indeed highly conductive with conductance values of 3000–20000 S, which are higher than those of stable continents at the same depth by 1–2 orders of magnitude. It implies that there are likely widespread hot fluids in the mid-lower crust beneath the Tibetan Plateau. For instance, the high-conductivity anomalies of the maximum values are found near the Yarlung Zangbo River in Southern Tibet and northern Qiangtang terrain in Northern Tibet, respectively. These significant results have been presented in the journal *Science* in 1996 (No. 274) [8, 9] and 2001 (No. 292) [10].

The aforementioned investigations are, however, primarily confined to the middle plateau in NS direction, not sensitive to variations of the lithospheric structure in EW direction. On the other hand, the widespread NS trending rifts within the plateau [11, 12] might imply that there should be drastic changes of electrical structure in EW direction. This issue should be addressed by field observations, which is of significance for the studies of deformation of the plateau.

Therefore, we deployed four profiles in NS direction across the Yarlung Zangbo River and one profile in EW direction for super-broadband MT sounding in 2001 and 2004, which are expected to reveal the electrical structure of crust and upper mantle in Southern Tibet.

In this paper, we use the imaging results of the above five MT profiles and one previous profile (line 100) to describe and analyze variations of electrical structure of lithosphere in both EW and NS directions around the Yarlung Zangbo River.

1 Field survey

This work began in 2001 and was completed at the end of 2005, during which two campaign surveys were conducted in the field.

1.1 Deployment of survey lines

As shown in Figure 1, five MT profiles in NS direction across the Yarlung Zangbo River were deployed in Southern Tibet. They are the Yatung-Xoggola (line 100) completed in 1995, Tsona-Medrogongkar (line 700) and Kyirong-Tsochen(line 800) in 2001, and Tingri-Comai (line 900) and Lower Zayu-Chamdo (line 1000) in 2004. In addition, the Lhaze-Markham profile (line 2000) is in EW direction.

Among them, line 100 is 250 km long with 31 broadband MT sites and 15 long-period (LIMS) MT sites, line 800 is 230 km long with 22 broadband sites and 9 LIMS sites, line 900 is 218 km long with 23 broadband sites, line 1000 is 280 km long with 24 broadband sites, and line 2000 is 1046 km long with 39 broadband sites.

Because of highly varying terrain and extremely bad traffic conditions, the MT sites were arranged with unequal intervals. In general, the site spacing is no more than 15km in NS profiles and less than 30 km in the EW profile. West to Chushur (site number 2034), the survey line is along the southern bank of the Yarlung Zangbo River, while east to

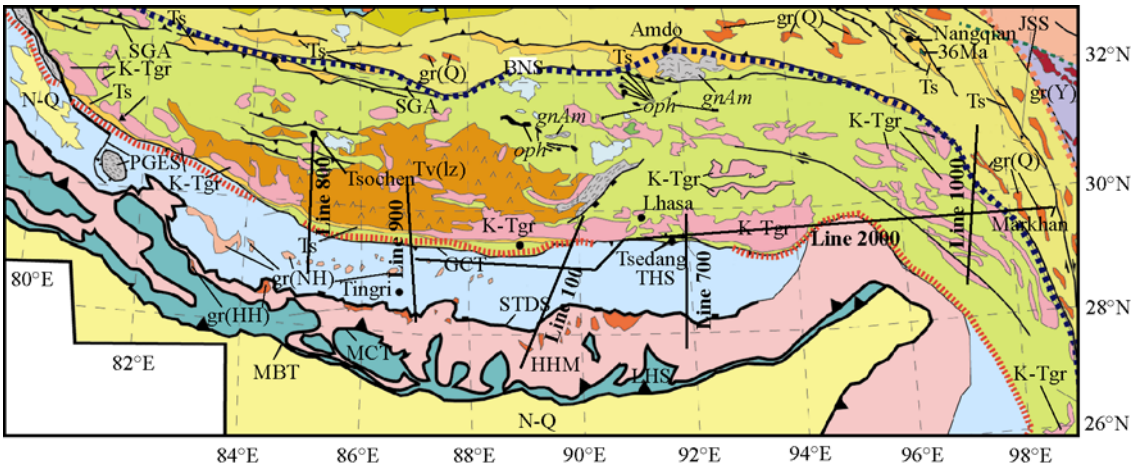

Figure 1 Sketch map showing magnetotelluric sounding profiles in Southern Tibet (base map from Yin [13]).

Chushur, it is along the northern bank, since the Yarlung Zangbo River turns toward south at site 2066.

Geographical coordinates of all the sites were determined precisely by the portable GPS receiver with errors less than 100 m. To assure a successful MT survey, advanced equipment and data processing methods were used as presented below.

1.2 Instrument and equipment

In previous MT surveys in China, the minimum frequency of observed signal is 0.0005 Hz, which limits the probing depth in Tibet where the crust is very thick. Thus, the periods of MT signal should be as large as tens of thousands of seconds for this work. Besides, the special tectonic evolution in Tibet has resulted in very complicated shallow and deep structures. To suppress distortion of shallow local structure and non-uniform electrical bodies, the MT signal of as high as several hundreds Hz is needed. In order to meet such a requirement, we chose the imported MT system of MT-24NS local network type made by EMT Co. of US, matched by the long-period intelligent system (LIMS) for the survey.

1) MT-24NS. During data acquisition in 2001 and 2004, two sets of the MT-24NS system were applied, which has sensitivity to the electric field of 0.02 μV/m, sensitivity to the magnetic field of 0.3 V/nT, and frequency range of 3.2×10^{2}– 4.6×10^{-4} Hz. By using this system, two horizontal components *Ex* and *Ey* of the electric field and three components *Hz*, *Hy*, and *Hx* of the magnetic field can be measured in time series simultaneously. Meanwhile, GPS data acquisition can be made at varied sites synchronously so that the MT remote reference technique can be implemented to enhance the quality of data acquired.

2) LIMS. Currently, the LIMS MT system is the best equipment for observations of super-long period MT signal. In 2001, 14 sets of this system were used for MT survey, which were provided by the partners of US and Canada.

Like the MT-24NS system, the LIMS system measures time series of five components of the electric and magnetic fields simultaneously, and employs the remote reference technique by means of GPS. Its sensitivity to the electric field is 0.02 μV/m, and that to the magnetic field is 100 nT/V, with frequency range of $0.1–3\times10^{-5}$ Hz.

1.3 Observation method

As mentioned above, the research of lithosphere structure in Tibet requires super-broadband MT data to be acquired. Thus, we have used the broadband MT-24NS system and long-period LIMS system in a combination manner. At a site, firstly broadband signals were measured by MT-24NS system at sampling rates of 1000, 60 and 15 Hz to form time series of 1 min, 1 h and more than 20 h respectively. Then, with the same electrode system, long-period signals were measured by LIMS system at rates of 1 and 0.2 Hz to produce time series of 2–3 weeks. After processing of the time series, the data in the frequency domain from two sets of MT systems were linked by using the Rhoplus method to generate MT response data of super-broadband (3.2×10^{2}–3×10^{-5} Hz), as shown in Figure 2.

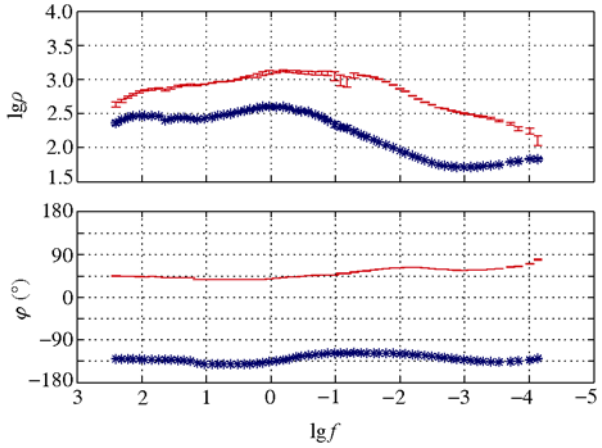

Figure 2 Super-broadband magnetotelluric sounding curves (MT-24+ LIMS). Red curve: *xy* mode; Blue curve: *yx* mode. ρ and f are in $\Omega\cdot$m and Hz, respectively. The same below.

This method requires that the data at same frequency points from the two systems are comparable, i.e., the data are of high quality. Hence, data acquisition must follow the relevant rules strictly and use the remote reference technique.

To achieve enough depth of exploration, super-broadband measurements were made for every one of two sites along a survey line to collect long-period MT signal.

1.4 Quality of data

There are two standards to assess MT data quality. One is data error and the other is continuity of sounding curves (frequency response curves). In this work, we have restricted that for 80% or more of all the sites, those frequency points with apparent resistivity errors greater than 5% and impedance phase errors larger than 5° can not exceed 25% of the total frequency point number. As for the continuity of sounding curves, they should be clear and of good forms, with regular changes of apparent resistivity and impedance phase with frequency.

The obtained MT data have been examined according to the two standards above. The result shows that the 83% of all data meet the requirement, implying a good quality of data. This demonstrates that our field measurements are successful.

2 Data processing and inversion

With the development of modern MT technology, a set of

sophisticated procedures for MT data processing and many inversion methods are available, such as the Robust processing [14] of time series of MT components, Rhoplus analysis [15], decomposition of complex impedance tensors [16] for MT data processing, 2D rapid relax inversion (RRI) [17], 2D Oceam inversion [18], and 2D conjugate gradient inversion [19].

These methods have been applied to MT data processing and inversion (including MT-24 and LIMS data) obtained in Southern Tibet. In 2D inversion of the super-broadband MT data on lines 100, 700, 800, 900, and 1000, the three aforementioned inversion methods are employed separately in a repeated manner on the single-mode and double-mode. In conjunction with geological and geophysical data [20–36], we have made comparison and analysis to the models of electrical structure from these inversions, and concluded that the result of 2D conjugate gradient inversion on the TM mode is relatively acceptable. Figure 3(a)–(e) displays the inversion models of the five MT profiles, which exhibit the 3D features of lithosphere electrical structure in Southern Tibet.

Figures 4 and 5 show the fitting results by 2D conjugate gradient inversion on the TM mode for the profiles line 900 and line 1000, respectively. A comparison between the observed and calculated data indicates that they are analogous to each other. We have examined distributions of fitting errors on the cross sections and sites along the survey lines. It is found that for all frequency points of the sites, the maximum root-mean-square (rms) errors of fitting results for apparent resistivity and impedance phase are less than ±4, and those synthetic errors for all sites are less than 2.

Although the above inversion results can be used to infer the conductive structure of crust and upper mantle, they are not the exclusive standard because of the inherent multiple solutions of geophysical inversion. To construct a convincing model of electrical structure, a series of comparison and analysis should be performed based on geological data and other geophysical observations.

According to the classical MT theory, when the conductivity of subsurface media meets the 2D condition, only along the structural strike, the magnetotelluric field can be separated into uncorrelated two sets of "linear polarized waves". In this case, the strike and dip can be regarded as two orthogonal primary axes of electrical property. Geologically, east-west trending structures dominate in Tibet, and thus the electrical structure of crust is stable in EW direction. In the light of this consideration, for the five MT profiles across the Yarlung Zangbo Rvier, measurements were made with the x axis in NS direction and y axis in EW direction. In MT data processing and 2D inversion, the XY mode is defined as H polarization mode and YX as E polarization mode, respectively. Consequently, the derived 2D conductivity models along all these profiles exhibit primarily the variations of the EW trending structures along NS direction.

However, numerous investigations have demonstrated that there are NS or nearly NS trending faults in the Tibetan Plateau. Because of their influence, the conductivity of crust in the plateau has a strong anisotropy in EW and NS directions. In this case, there also exist two orthogonal primary axes of electrical property, in which the MT field can also be separated into two uncorrelated "linear polarized waves" [37]. To study these NS faults and lateral variations of EW orientated crustal structures, we have deployed the Lahze-Markham (line 2000) MT profile in EW direction.

Figure 6 shows the distribution of primary electrical axes of subsurface media derived from MT profile line 200 based on decomposition of impedance tensors. On this line, west to the site 2058, the two primary axes of electrical property of subsurface media are orientated in about 0° (NS direction) and 90°(EW direction), respectively; while east to it those are in 40° (NE-SW direction) and 130° (SE-NW direction), respectively. Given that the primary electrical axes of subsurface media in Southern Tibet are in nearly NS and EW direction, and our attention is focused on the NS trending structures, the coordinate system for observations is rotated by 90° in MT data processing. Then we make data inversion using the conjugate gradient method to construct the electrical structure model of crust and upper mantle along line 200 as shown in Figure 3(f).

Then forward calculation is made to fit the inversion model on the TM mode for line 2000 (Figure 7). Similarly, we have made a careful comparison between the observed and calculated data, and examined distributions of fitting errors on the cross sections and sites of the line (see Figure 3, the portion indicated by the arrow). These examinations demonstrate that the inversion model for line 2000 is highly convincible. This model (Figure 3(f)) indicates that the electrical structure of lithosphere in Southern Tibet is strongly nonuniform in EW direction, and characteristic signatures of several NS trending structures are visible.

3 Electrical structure of lithosphere in Southern Tibet

Figure 3 shows contours of resistivity on cross sections for lines 100, 700, 800, 900, 1000, and 2000, which reflect the quantitative relationship between the depth and subsurface conductivity. In this figure, horizontal axis is the profile line and longitudinal axis is depth. Red color means low resistivity values while blue means high resistivity values.

In general, tightly arranged and curved or distorted contours of resistivity are indicators of interfaces or faults between different conductive media. Sparse and stable distribution of contours may imply a steady and uniform electrical layer; fluctuation of contours along a profile likely marks the interface traces of electrical layers; distribution of contour values can reveal the structural characteristics of the

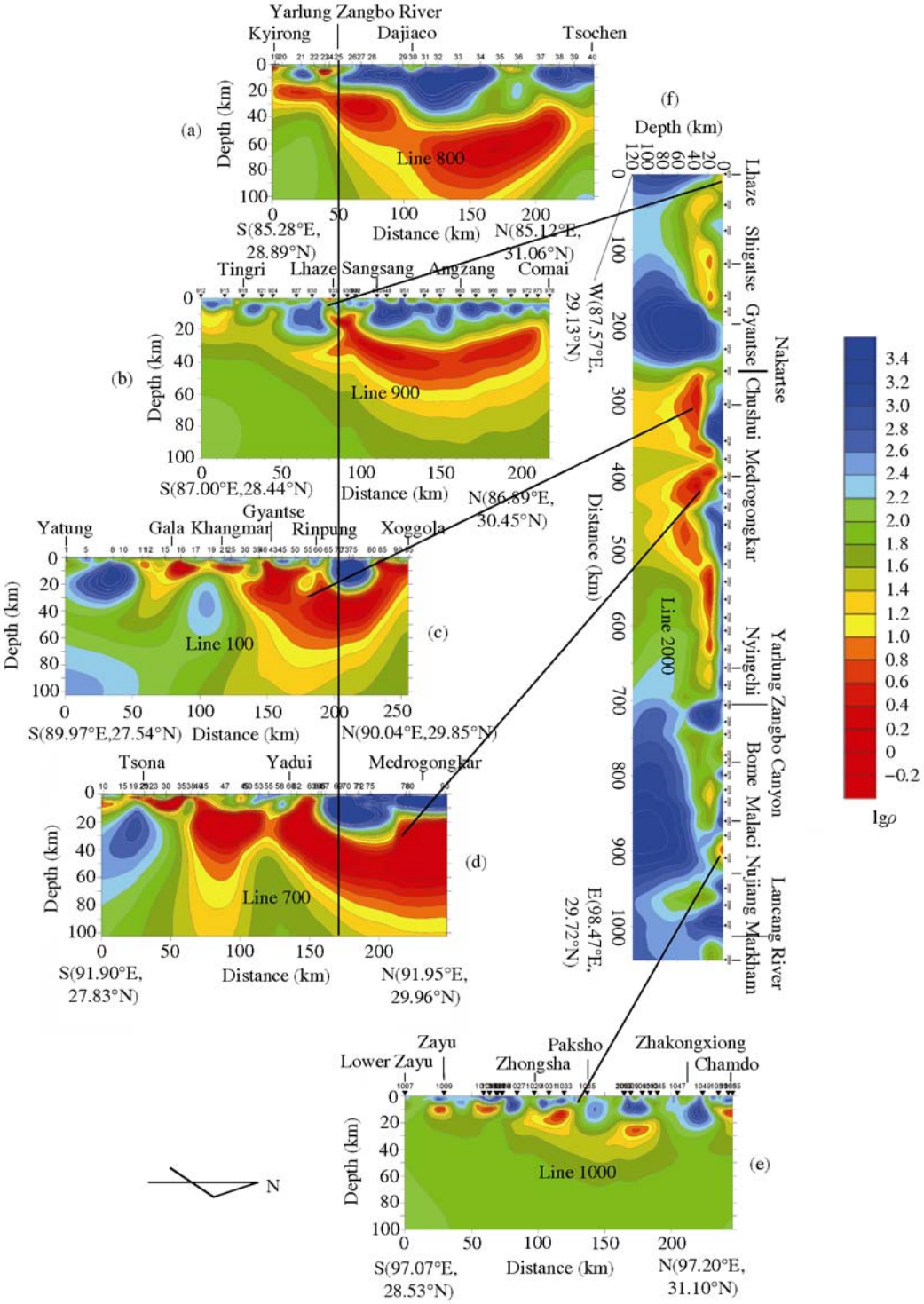

Figure 3 Lithosphere electrical conductivity models derived from MT data inversion in Southern Tibet. Arrows indicate intersection of profiles along the direction of south-north and east-west respectively.

electrical section. Therefore, based on images of resistivity contours on cross sections, we can construct models of electrical structure to describe the distribution of subsurface resistivity along survey lines.

Assume that the average resistivity of lithosphere in Tibet is 10 Ω·m. According to the calculation equation for penetration depth of a plane wave filed in isotropic medium, $H = \sqrt{10\rho T}/2\pi$ [37], the penetration depth of an MT signal of a period about 20000 s will exceed 225 km. It means

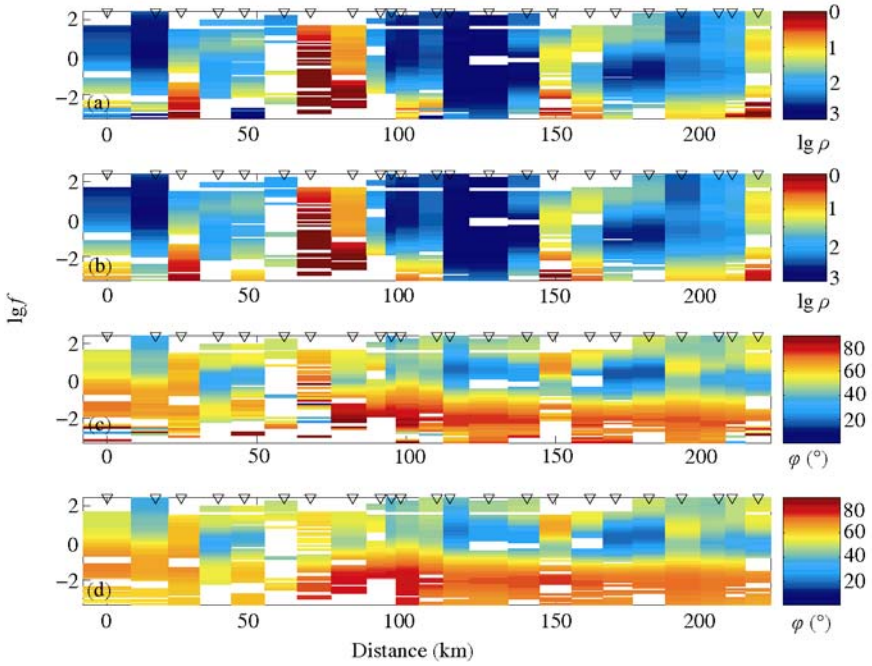

Figure 4 Fitting results of profile line 900 by MT data inversion on TM mode. (a) Observed apparent resistivity on TM mode; (b) calculated apparent resistivity by inversion on TM mode; (c) observed impedance phase on TM mode; (d) calculated impedance phase by inversion on TM mode.

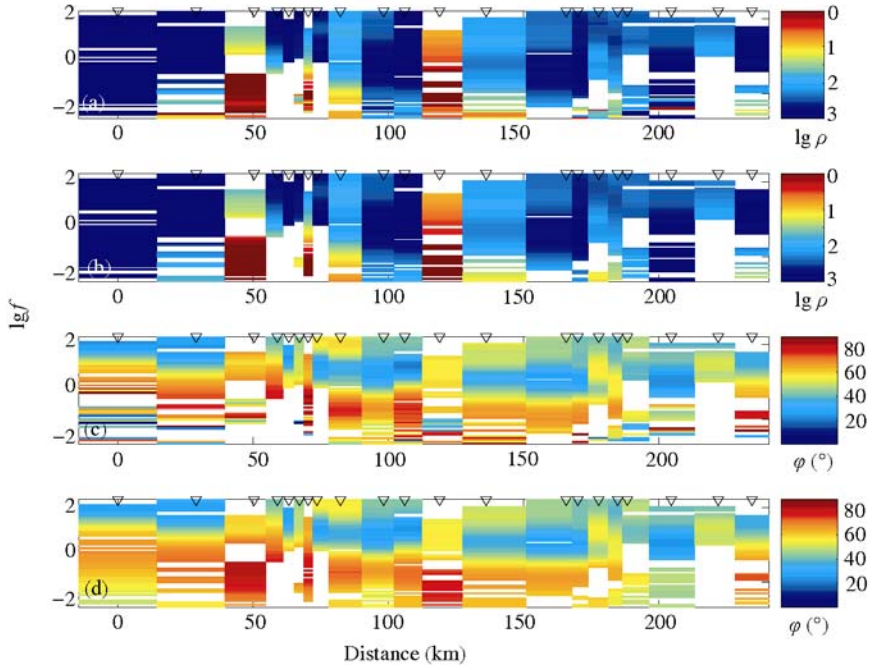

Figure 5 The same as Figure 4 but for profile line 1000.

that the maximum sounding depth of the MT surveys in Southern Tibet can reach this value. But considering the complexity of the actual subsurface media and other factors, we only use the inversion results above depth 100 km when discussing the features of electrical structure of the study area. Description is made for each profile below.

3.1 NS trending profiles across the Yarlung Zangbo River in Southern Tibet

3.1.1 Kyirong-Tsochen profile (line 800)

Figure 3(a) shows the 2D MT model computed by conjugate gradient inversion on the Kyirong-Tsochen profile. It

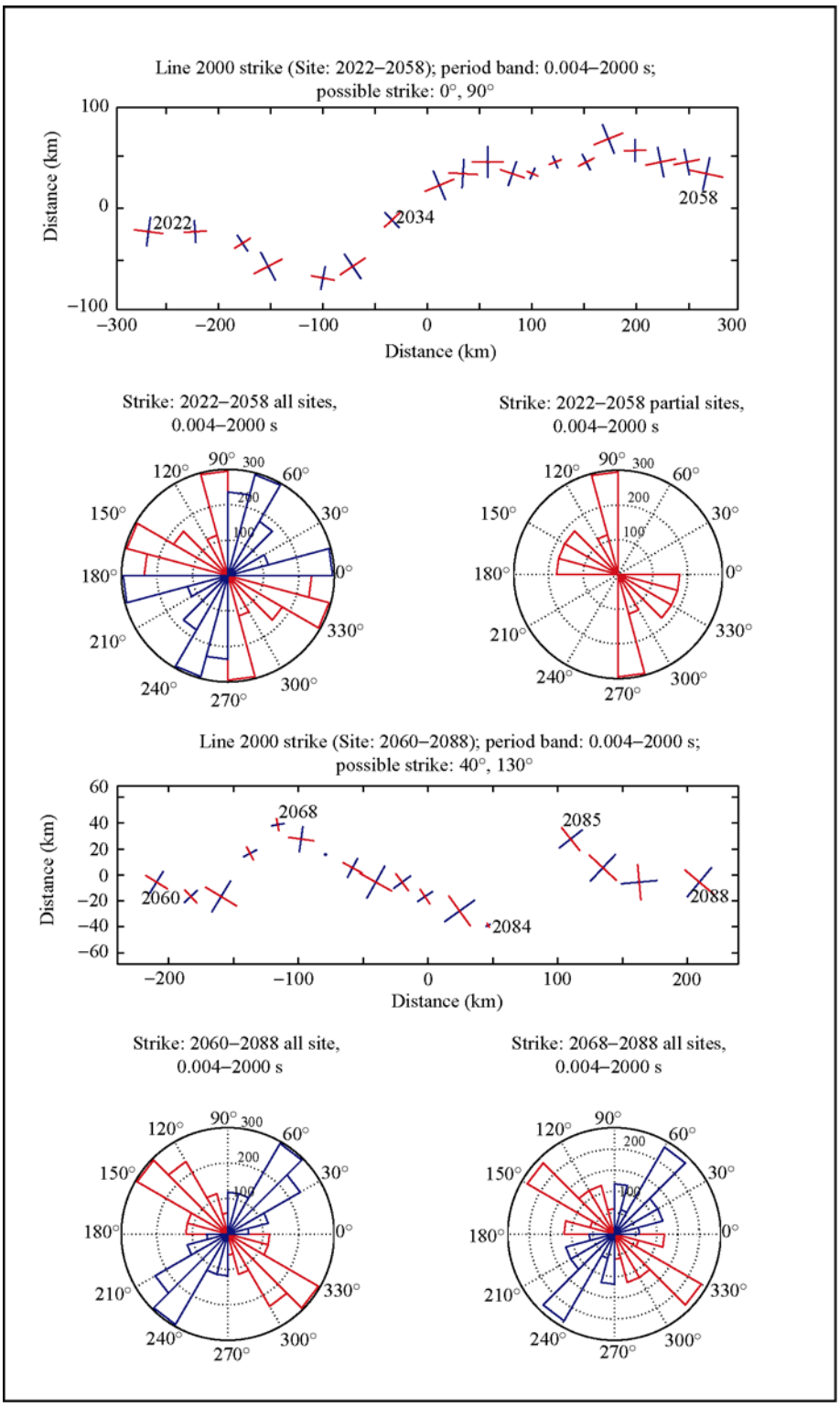

Figure 6 Distribution of primary electrical axes of subsurface media derived from MT profile line 200.

exhibits the conductivity structure of crust and uppermost mantle above depth 100 km in this area (85.28°E, 28.89°N–85.12°E, 31.06°N).

The cross section in this figure indicates that between Kyirong and Tsochen, the upper crust is of high resistivity with values of 200–3000 Ω·m. The top of this high-resistivity area exposes in a broad range, and its bottom lies at depths of 15–20 km. Between sites 30 and 35, the bottom is concave downward to depth 30 km. Toward north, the bottom of this high-resistivity area becomes shallow.

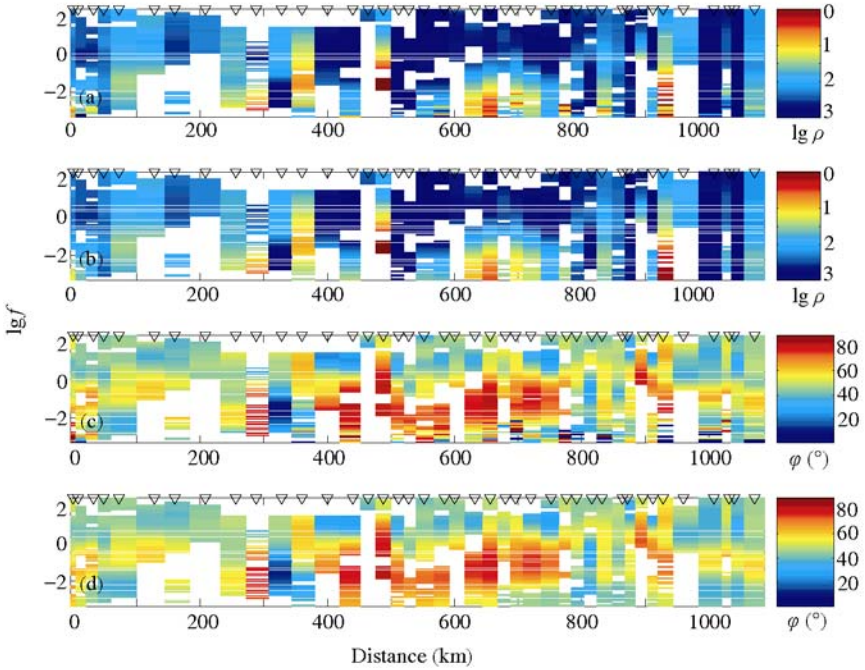

Figure 7 Fitting results of MT data inversion model on TM mode for profile line 2000.

South to the Yarlung Zangbo River, around sites 19–20 and 22–25, and north of sites 35 and 36, there are small-scale local high-conductivity bodies in the upper crust with resistivity values less than 10 Ω·m, of which the top is at depths of 3–5 km and bottom at depths of 7–10 km.

From south to north along the profile, a set of electrical gradient zones are present in the depth range of 15–45 km below the surface. Downward further is a high-conductivity layer in the mid-lower crust with resistivity less than 10 Ω·m. Its bottom is concave downward, centered between sites 32–34 with depth up to 100 km.

Globally, the top surface of the high-conductivity layer dips north. South to the Yarlung Zangbo River, it is thin and of gentle occurrence, situated in the middle crust. Northward crossing the Yarlung Zangbo River and entering the Lhasa-Gangdis terrane, most of this layer lies in the lower crust with a downward-concave form, of which the center tends to extend to upper mantle. Beneath this high-conductivity layer in the mid-lower crust, resistivity increases with depth and has intermediate values.

Apparently, around this profile the electrical structure of lithosphere is characterized by layering in depth direction and block division in north-south direction. On the profile, the main part of the high-conductivity layer in the mid-lower crust lies in the Lhasa-Gangdis terrane with deep top and large thickness.

3.1.2 Tingri-Comai profile (line 900)

This profile is located about 170 km east of line 800 (Figure 1). Its 2D electrical structure model is shown in Figure 3(b). In this area (87.00°E, 28.44°N–86.89°E, 30.45°N), the upper crust is largely of high resistivity of 100–3000 Ω·m with a top exposed on the surface, and a concave bottom downward to the maximum depth of 30 km on the northern bank of the Yarlung Zangbo River and between sites 954–960. Its structure appears more complex than that of line 800, as indicated by a series of crossing southward-dipping and northward-dipping gradient zones, which cut the high-conductivity layer into many discontinuous blocks. Thus, the upper crust in Southern Tibet, especially south of the Yarlung Zangbo River, exhibits a structural feature of "fault-bounded blocks".

South to the Yarlung Zangbo River, two small high-conductivity bodies in the upper crust are found near the sites 918 and 933 with resistivity less than 10 Ω·m. Compared with line 800, they look relatively smaller and shallower.

On this NS trending profile, beneath the upper crust of high-resistivity, a large-scale high-conductivity layer also exists in the mid-lower crust with resistivity less than 10 Ω·m. Its shape is like that on the profile line 800 with a concave center between sites 954–960 north to the Yarlung Zangbo River, tending to spread to upper mantle.

South to the Yarlung Zangbo River, the thickness, occurrence, and depth of the high-conductivity layer in the mid-lower crust are similar to those of line 800, but with higher resistivity of 20–100 Ω·m. Toward north, this layer turns thinner and shallower, and the main part is also in the Lhasa-Gangdis terrane.

In a general view, the electrical structure of lithosphere

along the Tingri-Comai (line 900) has also the feature of layering in vertical direction and block division in NS direction. But it is much more complex than line 800, especially south of the Yarlung Zangbo River where the upper crust has more deep faults. The large-scale high-conductivity layer in the mid-lower crust is similar to that on the profile line 800 except for smaller thickness and a shallower top.

3.1.3 Yatung-Xoggola profile (line 100)

About 200 km east of line 900 is this profile (88.97°E, 27.54°N–90.04°E, 29.85°N) (Figure 1), along which data acquisition for super-broadband MT sounding was completed for the first time in 1995. Using these data, the 2D electrical structure model was reconstructed by the conjugate gradient inversion (Figure 3(c)).

Compared with lines 800 and 900, the electrical structure of crust and upper mantle along this profile is analogous. The upper crust is of high-resistivity 150–3000 Ω·m. The bottoms of two anomalous bodies found near Pagri (between sites 8–10) and at the northern bank of the Yarlung Zangbo River (between sites 65–80) are 38 km and 25 km deep, respectively. For the rest portion, the bottom of the high-resistivity layer in the upper crust is largely in the depth range of 3–8 km. Clearly, its thickness is much smaller than that along the profiles lines 800 and 900. Thus, the top of the large high-conductivity body in the upper crust is also relatively shallower, about 5–25 km deep.

On this profile, the large-scale high-conductivity layer in the mid-lower crust consists of many distinct high-conductivity bodies, which are like those on the profiles lines 800 and 900 in shape and resistivity values. The maximum bottom depth of this layer is almost 70 km near site 55, and has a tendency to extend to upper mantle.

The primary part of this high-conductivity layer is located north to site 35 (near Gyantse), unlike the areas around lines 800 and 900 where the high-conductivity layer in the mid-lower crust is bounded by the Yarlung Zangbo River (see Figure 3(c)). South to site 35, three isolated high-conductivity bodies are found with different sizes in the upper crust, which are much larger than those on the profiles lines 800 and 900, located near sites 11–12, 15–17, and 19–30, respectively. Among them, the anomalous body near sites 15–17 is relatively bigger, with an associated low-resistivity zone extending to deeper crust.

Analysis of the electrical structure model indicates that the lithosphere in Southern Tibet, like the cases of lines 800 and 900, is also characterized by layering in vertical direction and block division in lateral direction. Compared with profiles lines 800 and 900, the top depth of high-conductivity layer in the mid-lower crust on the profile line 100 is decreased by large amplitude. Its primary part crosses the Yarlung Zangbo River and the southern boundary shifts toward south. And the size of the local high-conductivity body in the upper crust increases abruptly. These features are likely associated with the tectonic deformation in Southern Tibet.

3.1.4 Tsona-Medrogongkar profile (line 700)

This profile (91.970°E, 27.83°N–91.95°E, 29.95°N) lies 200 km east of line 100 (Figure 1). Figure 3(d) shows the 2D electrical structure model of lithosphere on this profile.

As a whole, the model is also subdivided into layers in vertical direction and blocks in NS direction. The upper crust is largely of high resistivity, of which the thickness is relatively smaller south to the Yarlung Zangbo River. It tends to become thinner toward south, though remains slightly thicker than that on the profile line 100. North to the Yarlung Zangbo River, the bottom of the high-resistivity body between sites 67–80 is 25 km deep.

In the mid-lower crust, there is also a large-scale high-conductivity layer, which is analogous to those on the three profiles in the west in shape and structure, but has a larger size than the line 100. Particularly, the high-conduc- tivity bodies in the upper crust between sites 10–15, 19–35 and 38–55 located in the south of Yarlung Zangbo River are much larger than those on lines 100, 900 and 800, with a slightly increasing depth of the top. For instance, the uppermost surface of the high-conductivity body between sites 38–55 is at depth 10 km, and its bottom is at depth more than 50 km. Its associated low-resistivity anomalous zone also exhibits a tendency extending toward upper mantle.

The southern boundary of the primary part of the high-conductivity layer aforementioned passes through site 55. Like the case on line 100, the primary part of this layer also crosses the Yarlung Zangbo River with a southward shifted southern boundary. And its bottom depth is as large as 90 km.

3.1.5 Conductive structure of lithosphere around the Yarlung Zangbo River in Southern Tibet

Based on 2D models of electrical structure on profiles lines 800, 900, 100, and 700 (Figure 3(a)–(d)), the conductive structure of lithosphere around the Yarlung Zangbo River in Southern Tibet can be summarized as follows:

1) This structure can be subdivided into blocks in NS direction and layers in vertical direction.

2) The upper crust is primarily of high resistivity media with values of 100–3000 Ω·m. Its thickness increases from south to north and becomes thinner abruptly from west to east between lines 900 and 100.

3) In the mid-lower crust, there exists a large-scale high-conductivity layer consisting of discontinuous bodies with resistivity values less than 10 Ω·m. In the west (lines 800 and 900) the southern boundary of the primary part of this high-conductivity lies near the Yarlung Zangbo River; while in the east (lines 100 and 700) it shifts to the southern bank of the river. It means that the primary part of this high-conductivity layer crosses the Tethyan Himalaya and Gangdis-Lhasa tectonic zone in the east, and is situated within the Gangdis-Lhasa tectonic zone in the west.

4) The top surface of the high-conductivity layer in the mid-lower crust fluctuates strongly, dipping from east to west and from south to north. It extends in EW direction for more than 1000 km and its primary part spans over 100 km in NS direction.

5) South to the Yarlung Zangbo River, there are many small high-conductivity bodies in the shallow upper crust. The mid-lower crust is dominated by intermediate conductivity with resistivity values of about 150 Ω·m, which grows with increasing of depth.

3.2 NS trending Lower Zayu-Chamdo profile (line 1000) in Southeastern Tibet

The Yalung Zangbo River does not flow through the "big bend" in Southeastern Tibet, 475 km east of line 700. Thus the NS trending Lower Zayu-Chamdo profile (line 1000) (97.07°E, 28.53°N–97.20°E, 31.10°N) does not cross this river, but instead cross the Nujiang and Lancang River (Figure 1). Figure 3(e) displays the 2D electrical structure model of lithosphere by conjugate gradient inversion on this profile. It exhibits much different features from the other four profiles in the west.

The contours of resistivity show that the upper crust has high-resistivity bodies of varied sizes with values of 90–3000 Ω·m, which are block-shaped and distributed in NS direction with increasing thickness from south to north. The depths of their bottoms vary in the range of 5–30 km.

In the middle crust there is a low-resistivity layer that comprises five sets of small and discontinuous high-conductivity bodies. This layer is asymmetric and concave downward along the profile. South of the profile (between sites 1007–1021) exist two sets of local high- conductivity bodies with resistivity less than10 Ω·m. Their upper boundary is 5 km deep and lower boundary is 12–16 km deep. In the middle of the profile (between sites 1027–1045), there are also two sets of high-conductivity bodies less than 10 Ω·m with top at depths of 10–20 km and bottom at depths of 25–40 km, which form the center of downward concave low-resistivity layer. The high-conductivity body at the northern end of the profile (between sites 1051–1055) has a top at depth of 10 km and bottom at depth of 20 km. Compared with other profiles, the sizes of the local high-conductivity bodies found in this area are relatively small.

Below the low-resistivity layer in the middle crust mentioned above, the crust has increasing resistivity with depth, varying from 30 to 180 Ω·m.

This profile indicates that the large-scale high-conductivity layer in the mid-lower crust found in the Yarlung Zangbo area, Southern Tibet, doses not extend to the "big bend" in Southeastern Tibet, where the probed high-conductivity layer in the middle crust likely does not belong to the high-conductivity of mid-lower crust widespread in the spread in the Tibetan Plateau.

3.3 EW trending Lhaze-Markham profile (line 2000) in the Yarlung Zangbo area

This profile begins from Lhaze in the west (87.57°E, 29.13°N), extending eastward to Markham (98.47°E, 29.72°N), 1046 km long. The survey line is on the southern bank of the Yarlung Zangbo River from Lhaze to Chushur and on the northern bank east to Chushur (Figure 1). Figure 3(f) shows the 2D electrical structure model of lithosphere on this profile, which exhibits a strongly non-uniform feature in EW direction.

From west to east along the profile, the crust and uppermost mantle can be roughly divided into four electrical sections of alternating high and low resistivity, which are bounded by sites 933–2028, 2028–2032, 2032–2066, and 2066–2088 (Figure 3(f)), and named as I, II, III, and IV, respectively. Among them, sections I and III are low resistivity and II and IV are high resistivity.

In section I, the upper crust contains intermediate resistivity bodies with values of 30–250 Ω·m, of which the thickness becomes thinner from west to east. In the middle crust, there is a low-resistivity layer comprising three discrete bodies with values less than 30 Ω·m, of which the uppermost surface is 8–12 km deep, dipping gently to west, and the bottom is 40–52 km deep. Its associated low-resistivity anomalous zone extends toward the lower crust.

In section II, high resistivity is present from crust to uppermost mantle with values about 3000 Ω·m.

Section III is the primary low-resistivity area around the Yarlung Zangbo River, Southern Tibet. Its eastern boundary coincides roughly with the big bend of the Yarlung Zangbo River. Within this section, the electrical structure of lithosphere is much more complicated than section I, exhibiting block-division in EW direction. In the vertical direction, contours of resistivity also show a feature of layered structure like the five NS trending profiles.

In this area the upper crust has a high-resistivity layer with 150–3000 Ω·m. Between sites 2032–2050, the thickness of this layer is highly variable with maximum 28 km between sites 2034–2036 and 2044–2046. From sites 2050–2066, the thickness of this high-resistivity is relatively stable, about 8 km.

A large-scale high-conductivity layer of less than 10 Ω·m is found in the middle crust, which consists of seven discrete bodies, featured by complex structure. The top surface of this layer changes much in the depth range of 8–40 km. And its bottom has highly changeable depths from 24 to 70 km. Between sites 2032–2050, the cross section of this high-conductivity looks like "W" shape, while between sites 2050–2064, it is shallow and thin with a sub-horizontal occurrence. Near the big bend of the Yarlung Zangbo River, its resistivity grows to 25 Ω·m. And between sites 2032–

2050, the associated anomalous zone of low-resistivity also tends to extend into upper mantle.

Section IV, already entering the Sanjiang (three-river) bend area in Southeastern Tibet, is of high resistivity, characterized by a much more complex electrical structure than section II. From contours of resistivity on the profile, the crust can be divided into blocks in EW direction and layers in vertical direction. Here the crust and uppermost mantle are dominated by high and intermediate conductivity with resistivity of 25–3000 Ω·m. In the middle crust, no large-scale high-conductivity layer is found, except for four discrete anomalous bodies of low resistivity with 25–150 Ω·m, which are located nearby sites 2070–2082, 2085–2086 and 2088, respectively. These are all largely in agreement with situation on the profile line 1000.

Combining the MT sounding on line 2000 with those on lines 800, 900, 100, 700 and 1000, we found that the large-scale high-conductivity layer in the mid-lower crust of Southern Tibet is highly nonuniform in EW direction. It extends in EW direction over 1000 km with local discontinuities. Near the bend of the Yarlung Zangbo River, this layer is confined to the upper-middle crust with a stable top surface, shallow depth and small thickness, and almost horizontal occurrence, where resistivity increases. Eastward across the bend of the Yarlung Zangbo River, i.e., Southeastern Tibet, the mid-lower crust is of intermediate conductivity with several discrete local low-resistivity bodies. It means that stretching of the high-conductivity layer in the mid-lower crust is limited by the big bend of the Yarlung Zangbo River in Southern Tibet, unable to reach Southeastern Tibet. This fact is likely related with different generation mechanisms of the high-conductivity layers in the mid-lower crust in Southern Tibet and Southeastern Tibet.

Then we superimpose the electrical structure model on the profile line 2000 upon the tectonic map of Southern Tibet (Figure 8). We find that the high-conductivity body in section I coincides with the NS trending Shantsa-Tingkye deep fault, and those in section III are consistent with the Yangbajain-Yatung and Sangri-Tsona faults, respectively [11]. Because lines 900, 100, and 700 cross sections I and III separately (Figure 3), they reveal similar features of the corresponding high-conductivity layers in the mid-lower crust. It implies that the spread of this high-conductivity layer is associated with the NS trending faults in Southern Tibet.

4 High-conductivity bodies and partial melting in crust and rheology in Southern Tibet

The most prominent finding by MT survey in Southern Tibet is the existence of large-scale high-conductivity bodies in the mid-lower crust, which is seen on all MT profiles (Figure 3). As the earliest survey in the field, the MT profile along Yatung-Xoggola (line 100) shows that there are many discrete anomalous bodies of high-conductivity in the middle crust in this region, which have resistivity less than 10 Ω·m and top surface at depths of 15–20 km (Figure 3(c)). They are in agreement with the bright spots and top of low-velocity zones found by seismic exploration. These data suggest that the crust of Southern Tibet contains layers of partial melting or hot fluids which cause anomalies of high-conductivity [2, 7].

The later MT soundings on other profiles, lines 700, 800, 900, and 1000, have also confirmed the presence of this high-conductivity layer, of which the upper boundary is about 10–25 km deep, extending to the south and north of the Yarlung Zangbo River (Figure 3). Meanwhile, the MT sounding on line 1000 and 2000 indicates that the eastern boundary of this high-conductivity layer is roughly confined to the big bend of the Yarlung Zangbo River. It means that the probable partial melting or hot fluids in the crust converge at this position, i.e., 94.88°E, 30.01°N.

Although the cause of these high-conductivity bodies is still a debatable issue, the most plausible explanation is partially molten bodies or water-bearing hot fluids. For instance, the study of seismic reflection data suggests that the top of this high-conductivity may contain hot fluids [38]. Analysis of surface waves claims that it is related with a broad zone of partial melting [2]. Because water-bearing fluids can reduce the melting temperature of crust and high heat flows are present in Southern Tibet [39], it has been inferred that partial melting can occur at depths of 20–30 km in this region [40]. Thus, a combined model of a partially molten layer covered by water-bearing horizons is able to give a reasonable explanation for MT and seismic data [38, 41]. Besides, the geometry of the high-conductivity layer derived from MT survey is consistent with that of the partially molten layer predicted by the geodynamic model [40].

The inferred partial melt is at depths of 20–30 km in the crust south of the Yarlung Zangbo River. Based on laboratory measurements of resistivity on molten water-bearing granite, the melt condition of crust in Southern Tibet has been studied [42]. By assuming that the high conductivity anomaly is caused by partial melt in crust, under a good connection condition, the relationship between the resistivity of partially molten bodies and melt percentage for the resistivity range 0.1–0.3 Ω·m has been calculated [43, 44]. Based on this result, it can be estimated that a melt percentage 5%–14% is needed to account for the typical resistivity 3 Ω·m in the crust of Southern Tibet (Figure 9(a)).

Usually crustal flow requires a low viscosity of rock less than a threshold, which depends on the thickness of the flowing layer. It has been suggested that over 30% partial melt can provide a low enough viscosity of rock [44]. While laboratory observations have indicated that the partial melt of percentage 5%–7% can produce a connected net-

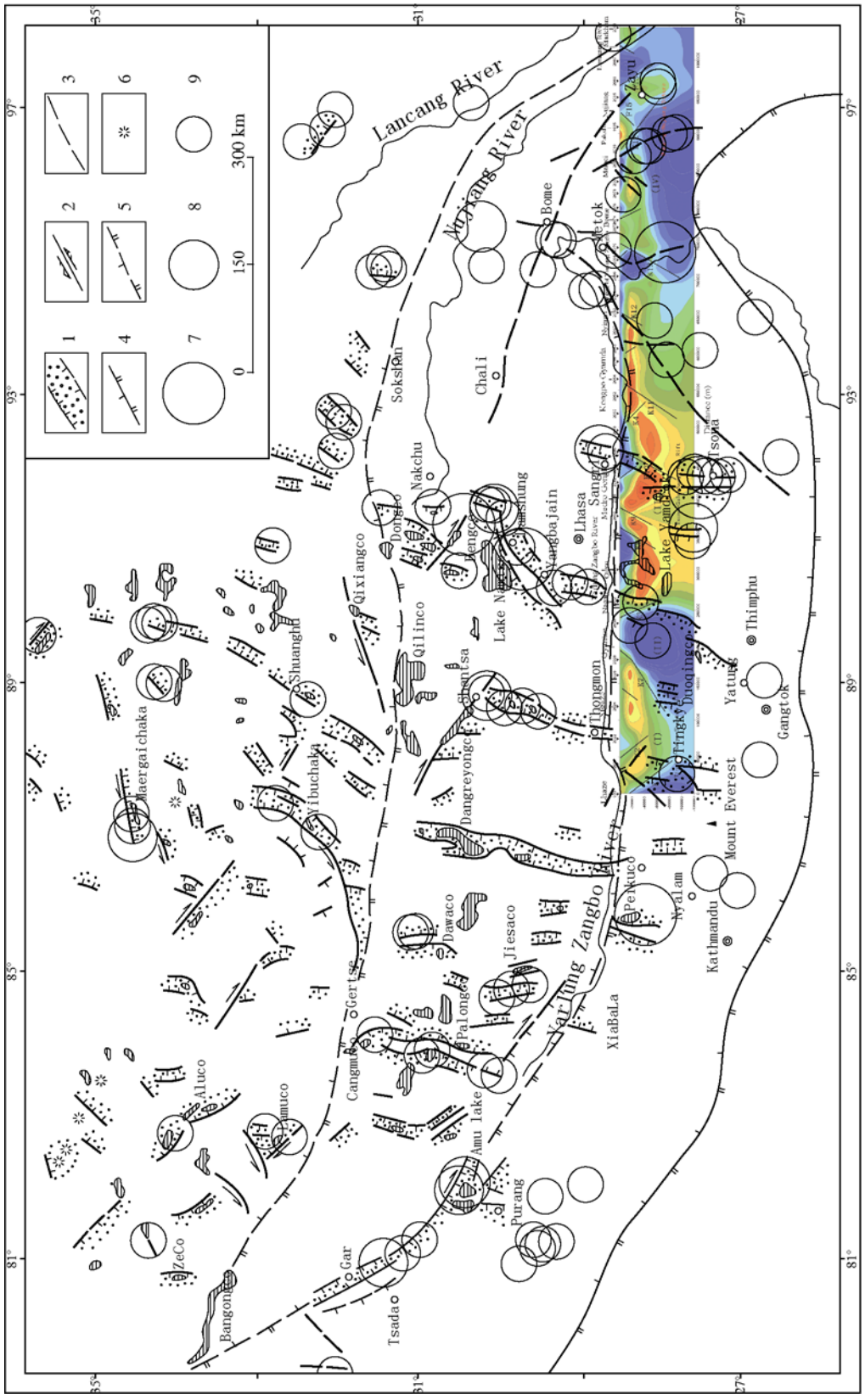

Figure 8 Tectonic map overlapped by electrical structure model of lithosphere on the MT profile line 2000 in Southern Tibet (base map from Han [11]). 1, boundary normal fault and depression zone; 2, strike-slip boundary fault; 3, inferred active fault; 4, siwalik main boundary fault zone; 5, early compressional deep fault; 6, Quaternary crater; 7, $M \geqslant 8$; 8, M=7–7.9; 9, M=6–6.9.

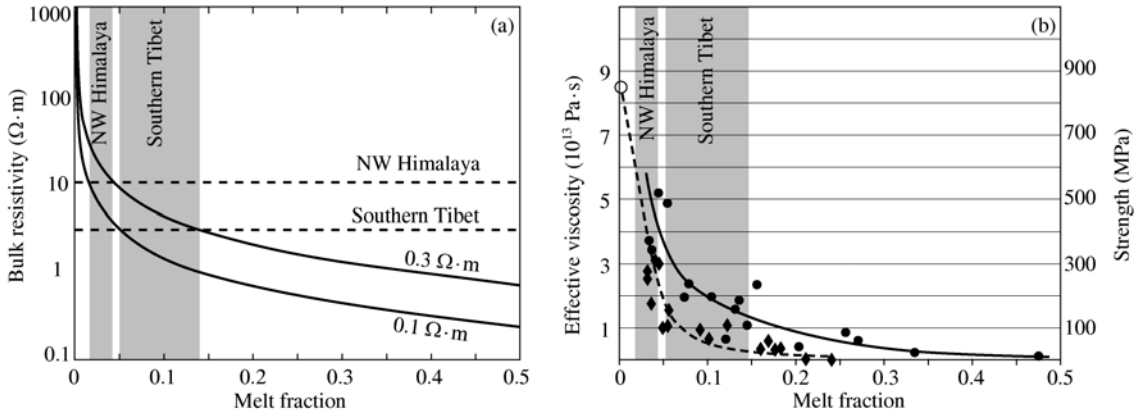

Figure 9 Summary of laboratory measurements of the electrical resistivity and mechanical properties of a partially molten rock (from Unsworth et al. [48]). (a) Bulk electrical resistivity of partial melts as a function of melt fraction for melt resistivities of 0.1 and 0.3 Ω·m; (b) effective viscosity and strength of Westerly granite (circles) and aplite (diamonds) as a function of melt fraction [45]. Error bars are not shown, and solid and dashed lines show best-fitting trends for these rocks [46, 47]. The strength was computed for a strain rate of 10^{-5} s^{-1}.

work which highly reduces the rock viscosity [45–47]. When the aplite sample has 0–7% partial melt, its effective viscosity is decreased by one order of magnitude [47]. This value is consistent with the dynamic model for Southern Tibet that claims channel flow in the crust [40].

As stated previously, the MT data suggests that the crust in Southern Tibet can have a partial melt up to 5%–14%. For the rock aplite, it can make viscosity reduced by one order of magnitude, which is much less than the viscosity needed by formation of the landform of the Tibetan Plateau (10^{16}–10^{18} Pa·s) [49], thus flow can occur in the crust. But for granite, this inference probably can not hold [46].

It should be noted that there is a great uncertainty in the extrapolation of viscosity of crust under low strain rates based on laboratory data (Figure 9(b)). Nevertheless, from MT soundings to mid-lower crust of low-viscosity, we can make inferences with dynamic implications.

5 Conclusions and discussion

On the basis of 2D electrical structure models on six MT profiles, this study attempts to describe the 3D features of lithospheric conductivity in Southern Tibet. It has been found that there is a widespread discontinuous high-conductivity layer in the mid-lower crust in a range spanning over 1000 km in EW direction. This layer becomes thinner, shallower with rising resistivity at the big bend of the Yarlung Zangbo River. Bounded by the Yarlung Zangbo River, the features of this high-conductivity are different between the east and west. West to the big bend of the river, the spread of this layer is associated with NS trending deep faults, implying different generation mechanisms. Based on the electrical models, this paper discusses the rheology of lithosphere in Southern Tibet. It is suggested that the high-conductivity in the mid-lower crust may indicate existence of partial melt and hot fluids. The thick crust in Southern Tibet contains warm, weak, and plastic materials in mechanics, which even can flow.

In conjunction with experiments of petrophysics, the MT data suggests that the partial melt in crust of Southern Tibet can reach 5%–14%. For aplite, this melt can make viscosity reduced to meet the flow condition of crust, but for granite, it cannot.

The result of this MT survey is important for the studies of some problems in the Tibetan Plateau, such as India-Eurasia collision, underthrusing models, deep structure, mechanisms of NS trending rifts, thermal state of crust, and probable crustal flow. It can also shed new light on resource exploration in Tibet, including minerals, oil and gas as well as geothermal fields. Of course, many complicated problems of geosciences remain to be solved by more field surveys and further research in the plateau, including deep structure and rheology of lithosphere this work is concerned.

This work was supported by National Natural Science Foundation of China (Grant No. 40674045) and National Special Project of China Sino-Probe-01.

1 Zhao W J, Nelson K D, Che J, et al. Deep seismic reflection evidence for continental underthrusting beneath Southern Tibet. Nature, 1993, 366: 557–559
2 Wei W B, Chen L S, Tan H D, et al. MT sounding on Tibetan Plateau—Electrical structure of crust and mantle along profile of Yatung-Bamucuo (in Chinese). Geosci J Graduate School China Univ Geosci, 1997, 11: 366–374
3 Wei W B, Chen L S, Tan H D, et al. An approach on subduction of Indian Plate from INDEPTH-MT results. Geoscience (in Chinese). J Graduate School China Univ Geosci, 1997, 11: 379–386
4 Wei W B, Chen L S, Tan H D, et al. Features of thermal structure and highly conductive bodies in middle crust beneath central and Southern Tibet: according to INDEPTH-MT results (in Chinese). Geosci J Graduate School China Univ Geosci, 1997, 11: 387–392
5 Wei W B, Tan H D, Deng M, et al. Conductivity of crust in Tibetan Plateau—Widespread fluids in the Tibetan crust found by magneto-

telluric detection. In: The 80th Annual Meeting Collections of Society of Chinese Geology (in Chinese). Beijing: Geological Publishing House, 2002. 487–493
6 Wei W B, Unsworth M, Jin S, et al. Conductivity structure of crust and upper mantle beneath the northern Tibetan Plateau: Results of super-wide band magnetotelluric sounding. Chin J Geophy, 2006, 49: 1098–1110
7 Wei W B, Jin S, Ye G F, et al. Features of faults in the central and northern Tibetan Plateau based on results of INDEPTH (III)-MT. Earth Sci China, 2007, 2: 1–8
8 Nelson K D, Zhao W J, Brown L D, et al. Partially molten middle crust beneath Southern Tibet: Synthesis of Project INDEPTH Results. Science, 1996, 274: 1684–1688
9 Chen L S, Booker J R, Jones A G, et al. Electrically conductive crust in Southern Tibet from INDEPTH magnetotelluric surveying. Science, 1996, 274: 1694–1696
10 Wei W B, Unsworth M, Jones A, et al. Detection of widespread fluids in the Tibetan crust by magnetotelluric studies. Science, 2001, 292: 716–718
11 Han T L. Himalayan Tectonic Evolution of Lithosphere-Tibet Tectonic Events (in Chinese). Beijing: Geological Publishing House, 1987
12 Zhou H W, Michael A, Murphy, et al. Tomographic imaging of the tibet and surrounding region: Evidence for wholesale underthrusting of Indian slab beneath the Tibetan Plateau (in Chinese). Earth Sci Front, 2002, 9: 285–292
13 Yin A. Himalayas-The Qinghai-Tibet Plateau orogenic geological evolution-Phanerozoic growth of the Asian continent (in Chinese). Acta Geosci Sin, 2001, 22: 195–229
14 Gber G D, Booker J R. Robust estimation of geomagnetic transfer functions. Geophys Roy Ast Soc, 1986, 87: 175–194
15 Weidelt P, Kaikkonen P. Local 1D interpretation of magnetotelluric B-polarization impedence. Geophys J Int, 1994, 117: 733–748
16 Gary W M, Alan G J. Multisite,multifrequency tensor decomposition of magnetotelluric data. Geophysics, 2001, 66: 158–173
17 Smith J T, Booker J R. Rapid inversion of two-and three-dimensional magnetotelluric data. J Geophys Res, 1996, 96: 3905–3922
18 Degroot-hedlin C, Constable S C. Occam's inversion to generate smooth, two-dimensional models from magnetotelluric data. Geophysics, 1990, 55: 1613–1624
19 Rodi W, Mackie R L. Nonlinear conjugate gradients algorithm for 2-D magnetotelluric inversion. Geophysics, 2001, 66, 174–187
20 Molnar P, Tapponnier P. Cenozoic tectonics of Asian: Effects of a continental collision. Science, 1975, 189: 419–426
21 Tapponnier P. The Ailao Shan-Red Rive metamorphic belt: Tertiary left-lateral shear between Indochina and South China. Nature, 1990, 343: 431–437
22 Cui Z Z, Yin Z X, Gao E Y, et al. Crustal structure of Qinghai-Tibet Plateau and its relationship with the earthquake (in Chinese). China Geol Acad Sci, 1990, 21: 215–226
23 Shen X J, Zhang W R, Yang S Z, et al. Heat flow evidences of different crust-mantle thermal structure in North-South terrain of Qinghai-Tibet Plateau (in Chinese). China Geol Acad Sci, 1990, 21: 203–214
24 Owenst T J, Zandt G. Implications of crustal property variations for models of Tibetan Plateau evolution. Nature, 1997, 387: 37–43
25 Kosarev G K R, Sobolev S V, Yuan X, et al. Seismic evidence for detached Indian lithosphere mantle beneath Tibet. Science, 1999, 283: 1306–1309
26 Kola-ojo O, Meissner R. Southern Tibet: Its deep seismic structure and some tectonic implications. J Asian Earth Sci, 2001, 19: 249–256
27 Cui Z Z, Yin Z X, Gao E Y, et al. Velocity Structure and Deep Tectonics of Qinghai-Tibet Plateau (in Chinese). Beijing: Geological Publishing House, 1992
28 Xiong S B, Liu H B, Yu G S, et al. Qinghai-Tibet Plateau lithosphere structure and tectonic study of artificial seismic. In: Pan Y S, Kong X R. Evolution of the Qinghai-Tibet Plateau Lithosphere Structure and Dynamics (in Chinese). Guangzhou: Guangdong Science and Technology Press, 1998. 1–35
29 Kong X R, Wang Q S, Xiong S B. Comprehensive geophysics and lithosphenc structure in the western Xizang (Tibet) Plateau. Sci China Ser D-Earth Sci, 1996, 39: 348–358
30 Zeng R S, Deng Z F, Wu Q J, et al. Seismological evidences for the multiple incomplete crustal subductions in Himalaya and Southern Tibet (in Chinese). Chin J Geophy, 2000, 43: 780–797
31 Li S H, Li M J, Unsworth M, et al. Partial melt or aqueous fluid in the mid-crust of Southern Tibet? Constraints from INDEPTH magnetotelluric data. Geophys J Int, 2003, 153: 289–304
32 Zhao G Z, Tang J, Zhan Y, et al. Relation between electricity structure of the crust and deformation of crustal blocks on the north eastern margin of Qiughai-Tibetan Plateau. Sci China Ser D-Earth Sci, 2005, 48: 1613–1626
33 Zhao Z D, Mo X X, Luo Z H, et al. Subduction of India beneath Tibet: Magmatism evidence (in Chinese). Earth Sci Front, 2003, 10: 149–157
34 Sun J, Jin G W, Dai D H, et al. Sounding of electrical structure of the crust and upper mantle along the eastern border of Qinghai-Tibet Plateau and its tectonic significance. Sci Chin Ser D-Earth Sci, 2003, 46(Suppl): 243–253
35 Ma X B, Kong X R, Liu H B, et al. The electrical structure of northeastern Qinghai-Tibet Plateau (in Chinese). Chin J Geophy, 2005, 48: 689–697
36 Zhao G Z, Chen X B, Wang L F, et al. Evidence of crustal 'channel flow' in the eastern margin of Tibetan Plateau from MT measurements. Chin Sci Bull, 2008, 53: 1887–1893
37 Shi Y J, Liu G D, Wu G Y, et al. A Course in Magnetotelluric Method (inChinese). Beijing: Geological Publishing House, 1985. 44–45
38 Makovsky Y, Klemperer S L. Measuring the seismic properties of Tibetan bright spots: Evidence for free aqueous fluids in the Tibetan middle crust. J Geophys Res, 1999, 104: 10795–10825
39 Armijo R, Tapponnier P, Mercier J L, et al. Quaternary extension in Southern Tibet: Field observations and tectonic implications. J Geophys Res, 1986, 91: 13803–13872
40 Beaumont C, Jamieson R A, Nguyen M H, et al. Himalayan tectonics explained by extrusion of a low-viscosity crustal channel coupled to focused surface denudation. Nature, 2001, 414: 738–742
41 Schilling F, Partzch G, Brasse H, et al. Partial melting beneath the magmatic arc in Central Andres deduced from geoelectromagnetic field data and laboratory experiments. Phys Earth Plan Int, 1997, 103: 17–31
42 Gaillard F, Scaillet B, Pichavant M. Evidence for present-day leucogranite pluton growth in Tibet. Geology, 2004, 32: 801–804
43 Li S, Unworth M, Booker J R, et al. Partial melt or aqueous fluids in the Tibetan crust: Constraints from INDEPTH magnetotelluric data. Geophys J Int, 2003, 153: 289–304
44 Renner J, Evans B, Hirth G. On the rheologically critical melt fraction. Earth Planet Sci Lett, 2000, 181: 585–594
45 Rosenberg C, Handy M R. Experimental deformation of partially melted granite revisited: Implications for the continental crust. J Metamorph Geol, 2005, 23: 19–28
46 Rutter E, Neumann D H K. Experimental deformation of partially molten Westerly granite under fluid absent conditions with implications for the extraction of granitic magmas. J Geophys Res, 1995, 100: 15697–15715
47 Van der Molen I, Paterson M S. Experimental deformation of partially molten granite. Contrib Mineral Petrol, 1979, 70: 299–318
48 Unsworth M, Jones A G, Wei W B, et al. Crustal rheology of the Himalaya and Southern Tibet inferred from magnetotelluric data. Nature, 2005, 438: 78–81
49 Clark M K, Royden L H. Topographic ooze: Building the Eastern margin of Tibet by lower crustal flow. Geology, 2000, 28: 703–706